ILASS–Europe 2017, 28th Conference on Liquid Atomization and Spray Systems, 6-8 September 2017, Valencia, Spain
*http://dx.doi.org/10.4995/ILASS2017.2017.*****

Role of heat transfer in bubble dynamics neglecting phase change. A numerical study

Stavros Fostiropoulos[*1,2,] , Ilias Malgarinos[1,2], George Strotos[3], Nikolaos Nikolopoulos[1], Emmanouil Kakaras[1], Phoevos Koukouvinis[2] and Manolis Gavaises[2]
[1]Centre for Research and Technology Hellas/Chemical Process and Energy Resources Institute (CERTH/CPERI), Egialeias 52, Marousi, Greece
[2]City University London, School of Engineering and Mathematical Sciences, Northampton Square, EC1V 0HB London, UK
[3]Piraeus University of Applied Sciences, Mechanical Engineering Department, 250 Thivon and P. Ralli str., Aegaleo 12244, Greece
[*]Corresponding author: fostiropoulos@certh.gr

Abstract
Bubble dynamics is generally described by the well-known Rayleigh-Plesset (R-P) equation in which the bubble pressure (or equivalently the bubble density) is predefined by assuming a polytropic gas equation of state with common assumptions to include either isothermal or adiabatic bubble behaviour. The present study examines the applicability of this assumption by assuming that the bubble density obeys the ideal gas equation of state, while the heat exchange with the surrounding liquid is estimated as part of the numerical solution. The numerical model employed includes the solution of the Navier-Stokes equations along with the energy equation, while the liquid-gas interface is tracked using the Volume of Fluid (VOF) methodology; phase-change mechanism is assumed to be insignificant compared to bubble heat transfer mechanism. To assess the effect of heat transfer and gas equation of state on bubble behaviour, simulations are also performed for the same initial conditions by using a polytropic equation of state for the bubble phase without solving the energy equation. The accuracy of computations is enhanced by using a dynamic local grid refinement technique which reduces the computational cost and allows for the accurate representation of the interface for the whole duration of the phenomenon in which the bubble size changes significantly. A parametric study performed for various initial bubble sizes and ambient conditions reveals the cases for which the bubble behaviour resembles that of an isothermal or the adiabatic one. Additional to the CFD simulations, a 0-D model is proposed to predict the bubble dynamics. This combines the solution of a modified R-P equation assuming ideal gas bubble content along with an equation for the bubble temperature based on the 1st law of thermodynamics; a correction factor is used to represent accurately the heat transfer between the two phases.

Keywords
Bubble dynamics, heat transfer, CFD-VOF model, 0-D model.

Introduction
The need for the inclusion of thermal effects in bubble dynamics was first addressed in [1] among others; it was shown that the polytropic gas assumption may provide inaccurate predictions of the bubble behaviour when thermal processes are taken into consideration. Since then, the effect of heat and mass transfer on bubble dynamics were examined in a large number of studies, either by CFD numerical models that are capable of solving the complex equations that characterize the physical processes of the bubble motion, or by reduced order models which include various assumptions but are computationally more efficient. In the framework of the CFD studies, the effect of heat transfer by solving the equation of gas-vapour bubble including variation of liquid temperature and assuming liquid incompressibility was examined in [2]. The main assumption in this study, was that the temperature distribution inside the bubble to be uniform, which allowed the authors to integrate analytically the continuity and momentum equations inside the bubble. In [3], the motion of a single bubble during a mild collapse was simulated, by solving the mass, momentum and energy equations when the ambient pressure increases stepwise. The authors highlighted the effect of heat and mass transfer on the bubble dynamics, while their main conclusion was that the mean bubble temperature and the decaying time of the bubble motion depend on the initial bubble radius. Regarding strong bubble collapses, where liquid compressibility has to be considered; the motion of a collapsing bubble subjected to a strong pressure field was investigated in [4] by using the Keller equation [5]. High pressure and temperature values at the collapse instant which are associated with the sonoluminescence, were observed
Regarding the reduced order models, in [6] thermal effects in bubble behaviour were investigated by using perturbation analysis method in the nearly adiabatic and isothermal regimes; the results are accurate only for very low Peclet numbers (isothermal limit). In high Peclet numbers, the model results in a convolution integral which is computationally expensive to be solved. In the context of sonoluminescence, a reduced order model has been proposed in [7]. Finally, a reduced order model has been developed in [8] by applying proper orthogonal

decomposition to the full set of equations for a spherical gas-vapour bubble, including heat and mass diffusion. A transfer coefficient, for heat and mass diffusion which directly depends on the Peclet number, was derived.
In the current study, the effect of heat transfer on bubble motion is examined by CFD, solving the energy equation and assuming that the bubble density follows the ideal gas equation of state. The detailed physical phenomena are analyzed based primarily on a CFD numerical model, the latter however used as well to propose an easily manageable in terms of computational cost 0-D model, following a sensitivity analysis among the 0-D and the CFD results.

Mathematical models

I. CFD numerical model

The bubble dynamics, for conditions that phase change is not considered, are investigated with a CFD simulation model which solves the Navier-Stokes equations in a 2-D axisymmetric domain along with the VOF methodology [9] to track the liquid-gas interface. For the simulations where heat exchange between the gas bubble (pure air bubble) and the surrounding liquid is considered, the energy equation is also solved and the bubble density is assumed to obey the compressible ideal gas equation of state. Additionally, for the evaluation of the heat transfer effects but also for validation purposes, CFD simulations were performed for the same initial conditions without solving the energy equation. For the latter cases, the bubble density obeys a polytropic gas equation of state ($p_g = \kappa\rho^n$), where the constant parameter κ is set according to a reference state for gas pressure p_g and density. The thermal VOF model has been extensively used in a number of studies from the authors' group in deforming droplet simulations such as in [10-12] and in [13-15], but also in cases with polytropic bubble dynamics as in [16, 17]. The model equations have been presented in detail in the aforementioned works and thus they are not repeated here. The present work is not considering any phase change effects and ignores any vapour presence (thus a pure air bubble is considered), any compressibility effects in the liquid phase, while the surface tension has been ignored since its effect is significant only for very small bubble sizes (nm). Additionally, the gas properties are kept constant (except of the density), without considering any dependence on temperature. Regarding the assumption of no phase change, this is proved to be true for the conditions examined (water at atmospheric conditions) since the thermodynamic parameter Σ proposed in [18] is small and bubble dynamics can be considered "inertially controlled". In any case, the aim of the present work is to isolate the effect of heat transfer on bubble dynamics and to propose a first basis for a 0-D model, while resulting to the fact that the results presented here cannot be directly related to the actual multi-phase actual phenomena appearing in bubble dynamics.
The 2-D axisymmetric computational domain is semi-circular and extends to a distance of 100 R_0 to minimize any influence of the boundary conditions on the solution. The computational cells are squares at the bubble region (1.5 R_0) and quadrilateral at the rest of the domain; this is shown in Figure 1. To enhance the accuracy of computations and achieve a low computational cost, an adaptive local grid refinement technique [19] is used. The grid resolution expressed as cells per Radius (cpR) range between 400 cpR for the maximum bubble radius and 8cpR for the minimum one. Far from the bubble, boundary conditions of constant pressure and temperature are applied, while only the half of the bubble is simulated by using symmetry boundary condition. The CFD simulations are performed with the commercial CFD tool ANSYS FLUENT v16 [20], along with various user defined functions (UDFs) for the implementation of the adaptive local grid refinement method in Malgarinos et al. [19] and the adaptive time-step for the implicit VOF solver.

II. 0-D model

Alongside with the CDF model, a 0-D model, which is capable of predicting the bubble size evolution under both pressure and thermal effects, is presented in this subsection. The model solves a modified Rayleigh-Plesset (R-P) equation along with an equation for the mean bubble temperature derived from an energy balance in the bubble. Apart from the aforementioned assumptions, the model further assumes uniform temperature and pressure inside the bubble, which are widely used in the works mentioned in the introduction. The present model is similar to the reduced order model in [8], which was derived by reducing the full set of equations using the proper orthogonal decomposition method (POD); nevertheless, the cases presented here correspond to different physical conditions, while Diesel liquid is also examined.

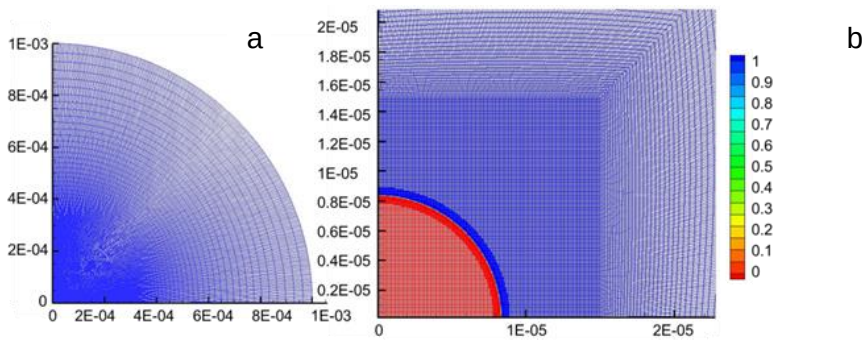

Figure 1. (a) Grid detail at the bubble region and (b) whole computational domain. Blue (red) colour indicates the ID of the gas (liquid) phase.

The classical Rayleigh-Plesset equation, which is an effective tool for the prediction of the bubble dynamic behaviour, is used as a starting point for the development of the 0-D model. In this study Rayleigh-Plesset equation is written as

$$\ddot{R} = \frac{1}{R}\left(-\frac{3\dot{R}^2}{2} + \frac{p_g - p_\infty}{\rho_l} - \frac{2\sigma}{\rho_l R} - 4\mu_l \frac{\dot{R}}{\rho_l R}\right), \qquad p_g = p_{g,0}\left(\frac{R_0}{R}\right)^3 \frac{T_{B,m}}{T_{B,m,0}} \tag{1}$$

Recall that the present work assumes a pure air bubble, thus the vapour pressure p_v is not appearing in eq. 1. In order to obtain an equation for $T_{B,m}$, the first law of thermodynamics for the bubble with ideal gas content is employed in the following form:

$$\dot{Q} - \dot{W} = m \cdot \left(c_v \frac{dT_{B,m}}{dt} + \frac{3}{5}\dot{R}\ddot{R}\right) \tag{2}$$

The first and second terms on the left hand side express the heat entering the bubble and the work done by the bubble, respectively. On the right hand side, m remains constant in the absence of phase change. The first and second terms inside the parentheses stand for the change of the mean internal energy and the change of the average bubble kinetic energy respectively; nevertheless, the second term can be ignored since it has been found to play a minor role conducting series of numerical tests. The formulation for the work done by the bubble is:

$$\dot{W} = p_B A_{surf} \dot{R}, \quad A_{surf} = 4\pi R^2 \tag{3}$$

Here, p_B is equal to p_g for the present cases. Finally, the most sensitive part of the present model is $\dot{Q}$. This is assumed to be equal to the product of $\dot{Q}_{ref}$ with a correction factor f_{heat} :

$$\dot{Q} = f_{heat}\dot{Q}_{ref}, \qquad \dot{Q}_{ref} = k_g \frac{T_\infty - T_{B,m}}{R} A_{surf} \tag{4}$$

More details on the heat flux will be further discussed in the next section. After substituting Eq. 3,4 into Eq. 2, the resulting model consists of a system of coupled O.D.E's (Eq. 1,2) which predicts the bubble dynamics when thermal effects are taken into account. The set of equation is integrated in time with a fourth order Runge-Kutta scheme.

Results and Discussion

I. Model results for an ideal gas bubble

In the first part of this section, results of the CFD ideal gas simulations are presented in Figure 2, along with those obtained from the commonly used assumption of polytropic gas bubble (either isothermal or adiabatic). In the ideal gas ones, the heat transfer between the bubble and the liquid is not predefined (adiabatic or isothermal), but becomes part of the solution. In Figure 2a, the case of bubble collapse ($p_\infty > p_{g,}$) is considered and the conditions examined are identical to those examined in [16] (p_∞ =10^5 Pa, $p_{g,0}$ =6900 Pa); for the ideal gas case, both the liquid and the gas have an initial temperature of 300 K. In Figure 2b, the case of bubble growth is considered (p_∞ =10^5 Pa, $p_{g,0}$ =$30{\cdot}10^5$ Pa); with an initial bubble temperature of 2500 K, higher than the initial liquid temperature. A first glimpse shows that the effect of heat transfer is quite important for the bubble expansion case compared to the bubble collapse one, while the ideal gas curve is not between the limiting conditions of isothermal and adiabatic behaviour as expected. Regarding the collapsing case (Figure 2a), the effect of heat transfer becomes more important after the first collapse and it is getting intensified as time evolves. These results are in agreement with previous studies in [6] and in [21] which state that not only pressure differences but also heat exchange between liquid and gas could affect bubble's behavior. Additional to the bubble radius behaviour, the temporal evolution of the mean bubble temperature is also of importance. The latter is shown in Figure 2c for the case of bubble collapse, where the differences at the bubble temperature profiles are more intense compared to those of the bubble radius. In the adiabatic regime, where there is no heat exchange between the gas and the liquid, there is a smooth variation of the mass averaged temperature in time and a high peak of 1800 K at the collapse instant is predicted from the 0-D model which for the moment neglects any heat transfer mechanism; in the isothermal regime the bubble is in thermal equilibrium with the surrounding liquid.

For the ideal gas case, the bubble temperature profile is located between the adiabatic and the isothermal regimes. For most of the time, the average bubble temperature is nearly constant and near the collapse there is a steep change of the mean temperature which reaches values up to 1120 K; this behaviour pertains to a rather isothermal bubble.

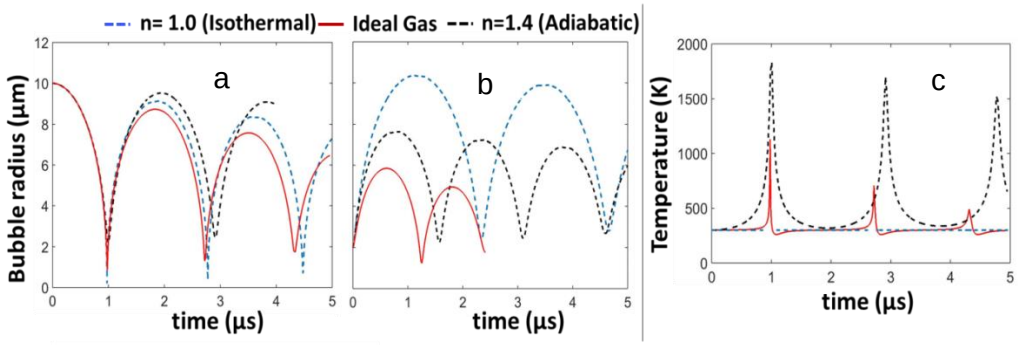

Figure 2. Results from CFD simulations: Bubble radius for collapse (p_∞ =10^5 Pa,$p_{g,0}$ =6900 Pa) (a) and growth (p_∞ =10^5 Pa,$p_{g,0}$ =3·10^5 Pa) (b) for the Ideal gas case, adiabatic case and isothermal case; c) temperature profile for the case of bubble collapse.

An interesting characteristic here is the cooling of the bubble below the liquid temperature, which is observed in the rebound right after the collapse. This occurs due to a time lag between the heat entering and the work received by the bubble [3]. This is a characteristic phenomenon that is captured also by the 0-D model.
The heat exchange between the gas and liquid can be quantified based on the CFD simulations by using Eq. 2, and solving for $\dot{Q}$. This is shown in Figure 3, which illustrates the temporal evolution of the heat flux at the bubble, which is smoothed by using a moving average filter, and the work done by the bubble normalized with the maximum absolute work value; the corresponding temporal evolution of non-dimensional bubble radius is also presented. During the collapse period, the work that the bubble receives from the liquid phase and the heat directed from the bubble to the liquid phase, increase in terms of absolute values, while upon collapse the work decreases abruptly. Later during the expansion phase, the bubble supplies work to the liquid and heat changes direction and flows towards the bubble. During the whole phenomenon, heat and work are in phase between them, while the ratio of their maximum absolute was computed equal to $\dot{Q}_{max}/\dot{W}_{max}$~0.2; the latter manifests the significance of heat transfer to the evolution of the phenomenon.
The analysis that follows in the rest of the paper concerns only cases of bubble collapse, while the reference operating conditions in [16] are used, as in Figure 2a. In order to relate the temporal evolution of $\dot{Q}$ provided by the CFD simulations (considered to be the actual one) with that of $\dot{Q}_{ref}$ (Eq. 4), a graph between the two is given in Figure 4a. Each collapse-expansion cycle is characterized by a circle-like trajectory which diminishes with time. The ratio of the aforementioned quantities provides f_{heat}, which works as a tuning parameter between the actual heat $\dot{Q}_{CFD}$, and the assumed expression for heat transfer ($\dot{Q}$) that has been used in the 0-D model (Eq. 4). In [8], it was found that the corresponding optimal correction factor is equal to 5 for a nearly isothermal behaviour; this parameter was kept constant during the simulation without making any distinction between the collapsing or the expanding phase. In this study the optimal f_{heat} value, which was found to be constant as well, is determined from the deviation between the CFD values and those predicted by the 0-D model for the bubble radius and the mean bubble temperature at the first collapse.

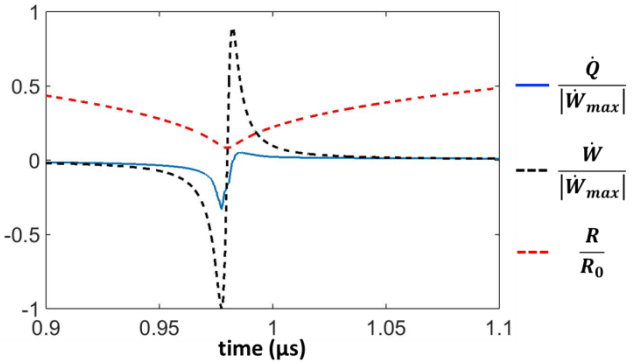

Figure 3. Evolution of the normalized heat (blue line), normalized work (black line) and bubble radius (red line) with time; results are demonstrated only for a time frame close to the bubble collapse.

The predicted deviation for a range of f_{heat} values is shown in Figure 4b. As seen, there is no value of the parameter f_{heat} resulting in a simultaneously optimum 0-D model performance for both the bubble radius and the temperature. The value chosen for the simulation is the one corresponding to the optimum performance in predicting the bubble radius, i.e. $f_{heat} = 10$. Additionally and judging from the error values, one could see in Figure 4b that the model performs well for a wide range of values of f_{heat} between 5 and 20. Next, the settings used in the CFD ideal gas case, are now implemented in the 0-D model. Figure 5 shows results of the 0-D model indicated by black solid line with $f_{heat} = 10$, against the results of the CFD ideal gas case. Note that there is a

deviation on the prediction of the maximum temperature value by the 0-D model compared to that by the CFD model equal to 218 K, however regarding the radius profile there is an identical match between 0-D model and CFD.

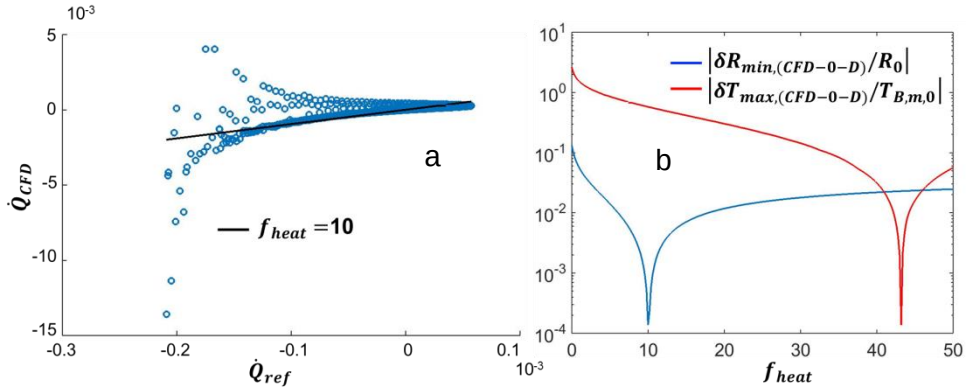

Figure 4. a) $\dot{Q}_{CFD}$ provided by CFD against $\dot{Q}_{ref}$ which is the assumed heat in the 0-D (blue scattered spots); constant correction factor $f_{heat} = 10$ (black solid line) .b) Deviation between the CFD values and those predicted with the 0-D model plotted in logarithmic scale for bubble radius (blue solid line) and temperature (red solid line) for various f_{heat} values.

II. Parametric study

In order to assess the effect of heat transfer on the bubble dynamics, a number of parametric cases with different properties and physical parameters, is performed. These include the effect of different initial bubble size and the effect of different ambient conditions with varying initial pressure difference, temperature and conductivity in both the liquid and the gas phase. The aforementioned parameters were varied with respect to the reference settings with the corresponding results to be always compared against the results of the reference case shown in Figure 5. It has to be mentioned that a limited amount of the examined cases will be presented in the context of this paper, for reasons of space limits. Figure 6 quantifies the bubble dynamics for various initial bubble radius (a) and initial liquid pressure (b). The results of the 0-D model show very good agreement with CFD for the parametric initial radius cases (a). The results of the cases with various initial pressure show rather satisfactory agreement (right panels).

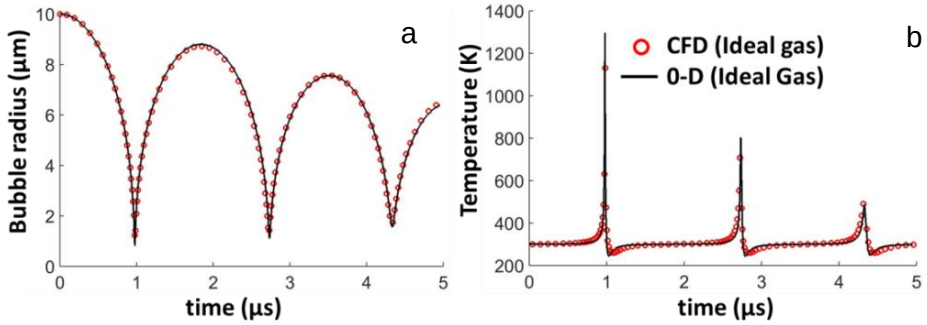

Figure 5. Radius (a) and temperature (b) profile of the CFD (red scatter) and 0-D model (black solid line).

Here, the examined case with increased liquid pressure ($2 \cdot p_\infty$) exhibits discrepancies, probably due to the fact that, for large pressure differences, the assumption of a uniform pressure is violated [22]. Regarding the examined temperature profiles which are not presented here, the 0-D model is not capable of capturing accurately the temporal evolution of bubble temperature. Particularly, in the examined case with increased liquid pressure, the deviation between the temperature peak predicted from the CFD and the 0-D model is quite high. Moreover, parametric runs with various liquid and gas conductivities were conducted. The corresponding results which are not presented in this study, reveal that the model used is able to capture all the cases examined and that the liquid conductivity is playing a minor role relative to the gas conductivity. Finally, the performance of the 0-D model is examined for liquid Diesel with properties computed from Kolev [23] at atmospheric conditions. Specifically, the properties assumed are the following; liquid density ($\rho_l = 826$ kg m^{-3}), heat capacity ($c_p = 1993.7$ J kg^{-1} K^{-1}), liquid thermal conductivity ($k_l = 0.12$ W m^{-1} K^{-1}) and liquid dynamic viscosity ($\mu_l = 0.003$ Pa s). Results show that the 0-D model with the same correction factor ($f_{heat} = 10$), is capable of capturing the behaviour of Diesel liquid (Figure 7), which exhibits lower peak temperature values and the bubble energy dissipates faster compared to water liquid due to its larger viscosity.

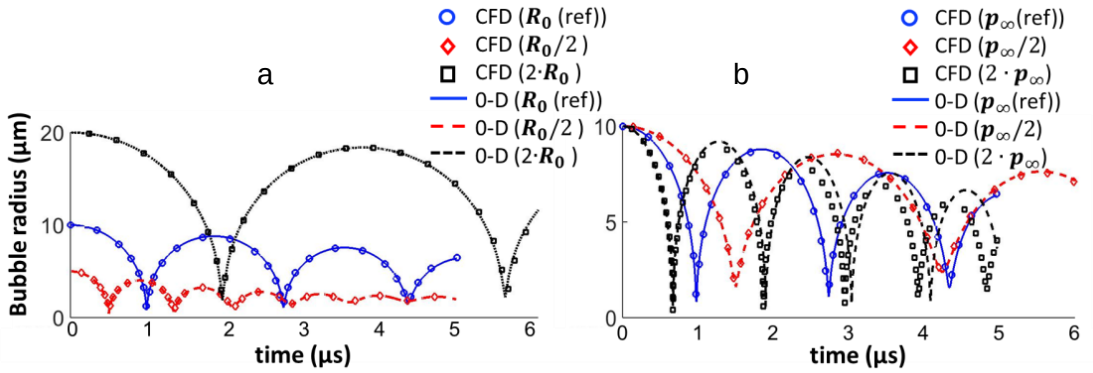

Figure 6. Bubble radius and temperature profiles for 0-D model (solid and dashed lines) against CFD (scatter spots) for parametric initial bubble radius (a) and initial liquid pressure (b).

In the last part of this subsection, quantification of the overall effect of heat transfer is carried out. For each parametric case the following factor is determined based on the minimum bubble radius only for the first collapse.

$$F_R = \frac{R_{min,thermal} - R_{min,n=1}}{R_{min,n=1.4} - R_{min,n=1}} \quad (5)$$

, where $R_{min,n=1.4}$ and $R_{min,n=1}$ are the minimum bubble radius at the adiabatic and the isothermal regime, respectively. The aforementioned factors range between 0 and 1. When factor values are closer to 0 the bubble motion is close to that of an isothermal bubble, while when they approach 1 the bubble tends to behave adiabatically.

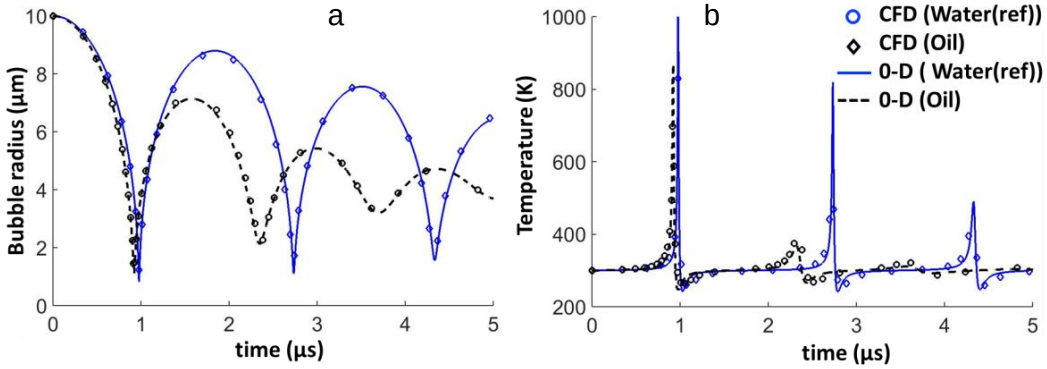

Figure 7. Bubble radius (a) and temperature (b) profile for the 0-D model (solid and dashed lines) against CFD (scatter spots).

The isothermal-adiabatic behaviour is evaluated against the gas phase Peclet number, which reads:

$$Pe_{g,ref} = \frac{R_0 u_{ref}}{a_{g,0}}, u_{ref} = \sqrt{3p_\infty/\rho_l} \quad (6)$$

Here, $a_{g,0}$ is based on a reference velocity u_{ref} which is derived from a bubble natural frequency used in [8]. Figure 8 shows the factors computed from both CFD and 0-D models (denoted as F_{R_CFD} and F_{R_0D} respectively) plotted against the $Pe_{g,ref}$ number. Regarding the bubble radius, it is clearly demonstrated that for the low Peclet number limit the bubble tends to perform isothermally, while for higher Peclet numbers the bubble motion approaches the behaviour of an adiabatic bubble. Moreover, it is demonstrated that in the range of Peclet number with values between 10^{-2} and 1, there is small deviation between the F_{R_CFD} and the F_{R_0-D}. On the other hand, for Peclet number larger than 1, it seems that the aforementioned deviations become more significant. Consequently, the proposed 0-D model with $f_{heat} = 10$, can provide reliable results for $Pe_{g,ref} < 1$.

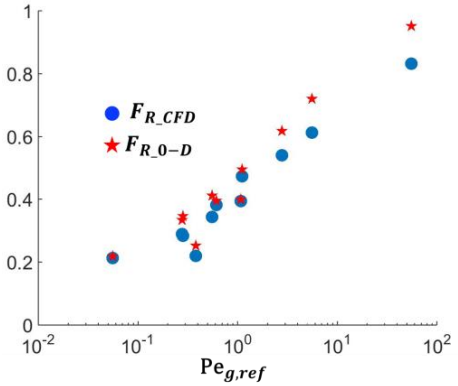

Figure 8. Computed factor from CFD and 0-D model for both minimum bubble radius.

Conclusions

In this study, the individual effect of heat transfer on bubble dynamics was examined by solving the energy equation and assuming that the bubble density follows the ideal gas equation of state, always targeting conditions where phase change can be neglected as in the considered cases where liquid temperature is not higher than 300 K. The detailed physical phenomena were investigated with a 2-D axisymmetric CFD numerical model coupled with the VOF methodology, while an adaptive local grid refinement technique enhanced the accuracy of computations with a low computational cost. Alongside with the CFD numerical model, a 0-D model that predicts bubble motion, is proposed. The latter combines a modified Rayleigh-Plesset equation along with an equation for the mean bubble temperature based on the first thermodynamic law. The model also requires the estimation of the heat flux towards the bubble. This was determined by processing the CFD data and it was modeled with a simplified expression using a constant tuning factor; nevertheless, this was found adequate to capture the basic physics and simulate with acceptable accuracy a wide range of cases. These include various bubble sizes, various bubble-liquid pressure differences and liquid/gas properties. Specifically, in the low Peclet number limit with values between 10^{-2} and 1, where bubble performs rather isothermally, the 0-D model is capable to provide reliable results due to the identical matching of the latter with the corresponding results from the CFD model. On the other hand, for Peclet numbers larger than 1, the 0-D model with the specific constant correction factor does not provide very accurate results, though more cases need to be examined. Finally, a future plan, related to the current study, is to examine the same phenomenon under evaporating conditions. For that reason further development of the 0-D model, with the inclusion of mass diffusion terms is needed.

Acknowledgements

Financial support from the MSCA-ITN-ETN of the European Union's H2020 programme, under REA grant agreement n. 675676 is acknowledged.

Nomenclture

Roman symbols

p	pressure [Pa]
T	temperature [K]
ρ	density [kg m^{-3}]
R	radius [m]
m	mass [kg]
A_{surf}	bubble surface area [m^{2}]
$\dot{W}$	rate of work [W]
$\dot{Q}$	rate of heat [W]
k	thermal conductivity [W m^{-1} K^{-1}]
c_p	isobaric heat capacity [J kg^{-1} K^{-1}]
c_v	isochoric heat capacity [J kg^{-1} K^{-1}]
Pe	Peclet number
n	polytropic exponent
F_R	isothermal/adiabatic factor
f_{heat}	correction factor

Greek symbols

σ	surface tension [N m^{-1}]
a	thermal diffusivity [m^{2} s^{-1}]
μ	dynamic viscosity [Pa s]
u	velocity [m s^{-1}]
κ	constant parameter

Subscripts

∞	far-field quantity
0	initial value
g	gas
l	liquid
v	vapour
B	bubble
m	mass-averaged
ref	reference value
CFD	values provided by CFD
0-D	values provided by 0-D

Dotted symbols

$\dot{\varphi}$	first time derivative
$\ddot{\varphi}$	second time derivative

References

1. Prosperetti, A., L.A. Crum, and K.W. Commander, *Nonlinear bubble dynamics.* The Journal of the Acoustical Society of America, 1988. **83**(2): p. 502-514.
2. Nigmatulin, R., N. Khabeev, and F. Nagiev, *Dynamics, heat and mass transfer of vapour-gas bubbles in a liquid.* International Journal of Heat and Mass Transfer, 1981. **24**(6): p. 1033-1044.
3. Matsumoto, Y. and F. Takemura, *Influence of Internal Phenomena on Gas Bubble Motion. Effects of Thermal Diffusion, Phase Change on the Gas-Liquid Interface and Mass Diffusion between Vapor and Noncondensable Gas in the Collapsing Phase.* JSME International Journal Series B, 1994. **37**(2): p. 288-296.
4. Vuong, V.Q. and A.J. Szeri, *Sonoluminescence and diffusive transport.* Physics of Fluids, 1996. **8**(9): p. 2354-2364.
5. Keller, J.B. and M. Miksis, *Bubble oscillations of large amplitude.* The Journal of the Acoustical Society of America, 1980. **68**(2): p. 628-633.
6. Prosperetti, A., *The thermal behaviour of oscillating gas bubbles.* Journal of Fluid Mechanics, 1991. **222**: p. 587-616.
7. Kreider, W., et al., *A reduced-order, single-bubble cavitation model with applications to therapeutic ultrasound.* The Journal of the Acoustical Society of America, 2011. **130**(5): p. 3511-3530.
8. Preston, A., T. Colonius, and C. Brennen, *A reduced-order model of diffusive effects on the dynamics of bubbles.* Physics of Fluids, 2007. **19**(12): p. 123302.
9. Hirt, C.W. and B.D. Nichols, *Volume of fluid (VOF) method for the dynamics of free boundaries.* Journal of Computational Physics, 1981. **39**(1): p. 201-225.
10. Strotos, G., et al., *Predicting the evaporation rate of stationary droplets with the VOF methodology for a wide range of ambient temperature conditions.* International Journal of Thermal Sciences, 2016. **109**: p. 253-262.
11. Strotos, G., et al., *Numerical investigation of aerodynamic droplet breakup in a high temperature gas environment.* Fuel, 2016. **181**: p. 450-462.
12. Strotos, G., et al., *Aerodynamic breakup of an n-decane droplet in a high temperature gas environment.* Fuel, 2016. **185**: p. 370-380.
13. Malgarinos, I., N. Nikolopoulos, and M. Gavaises, *A numerical study on droplet-particle collision dynamics.* International Journal of Heat and Fluid Flow, 2016. **61**: p. 499-509.
14. Malgarinos, I., N. Nikolopoulos, and M. Gavaises, *Numerical investigation of heavy fuel droplet-particle collisions in the injection zone of a Fluid Catalytic Cracking reactor, Part I: Numerical model and 2D simulations.* Fuel Processing Technology, 2017. **156**: p. 317-330.
15. Malgarinos, I., N. Nikolopoulos, and M. Gavaises, *Numerical investigation of heavy fuel droplet-particle collisions in the injection zone of a Fluid Catalytic Cracking reactor, part II: 3D simulations.* Fuel Processing Technology, 2017. **156**: p. 43-53.
16. Koukouvinis, P., et al., *Numerical simulation of a collapsing bubble subject to gravity.* Physics of Fluids, 2016. **28**(3): p. 032110.
17. Koukouvinis, P., et al., *Simulation of bubble expansion and collapse in the vicinity of a free surface.* Physics of Fluids, 2016. **28**(5): p. 052103.
18. Brennen, C.E., *Cavitation and bubble dynamics*. 2013: Cambridge University Press.
19. Malgarinos, I., N. Nikolopoulos, and M. Gavaises, *Coupling a local adaptive grid refinement technique with an interface sharpening scheme for the simulation of two-phase flow and free-surface flows using VOF methodology.* Journal of Computational Physics, 2015. **300**: p. 732-753.
20. Fluent, A., *Release 16.0, ANSYS*. 2014, Inc.
21. Nigmatulin, R. and N. Khabeev, *Heat exchange between a gas bubble and a liquid.* Fluid Dynamics, 1974. **9**(5): p. 759-764.
22. Storey, B.D., H. Lin, and A.J. Szeri, *Physically realistic models of catastrophic bubble collapses.* http://resolver. caltech. edu/cav2001: sessionB6. 001, 2001.
23. Kolev, N.I., *Thermodynamic and transport properties of diesel fuel*, in *Multiphase Flow Dynamics 4*. 2011, Springer. p. 293-327.

EDITORIAL UNIVERSITAT POLITÈCNICA DE VALÈNCIA